Supplemental Information for Larschan, Bishop *et al.*

X chromosome dosage compensation via enhanced transcriptional elongation in *Drosophila*

Supplementary Figures

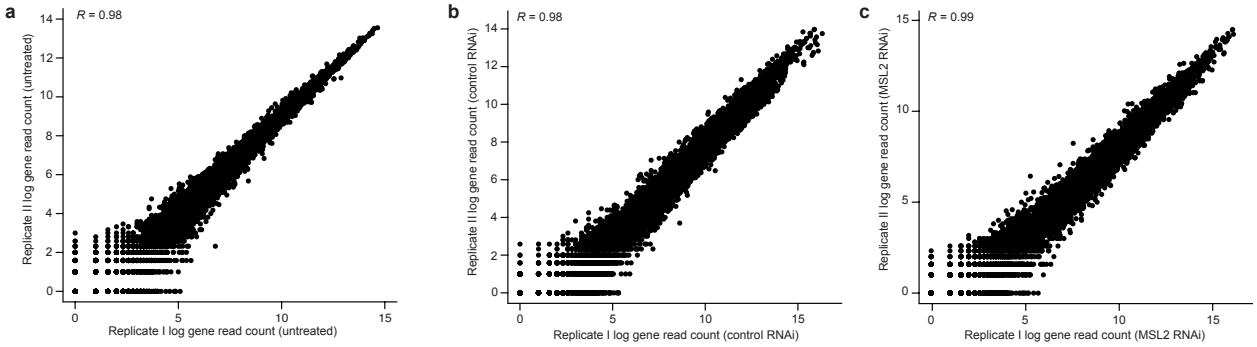

Figure S1. **Correlation of total tag counts per gene between replicates.** Total tag counts within each gene were computed for each replicate and plotted as a scatter plot in log scale (base 2). Pearson correlation coefficients between replicates are excellent (untreated: $R = 0.98$, control RNAi: $R = 0.98$; MSL2 RNAi: $R = 0.99$).

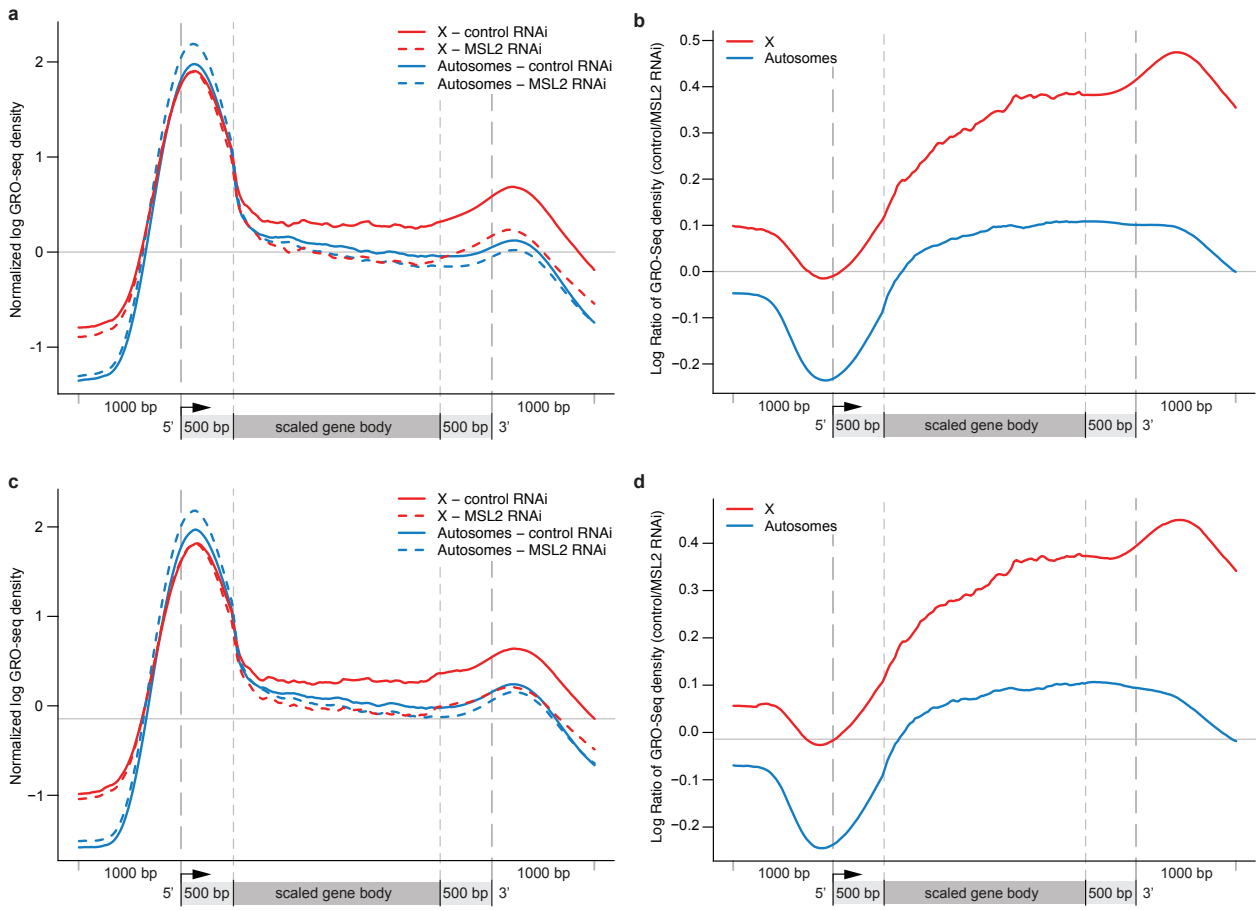

Figure S2. Filtering out the potential contribution of nearby genes or aberrant copy number does not alter the metagene profiles. **a** and **b**, To determine whether the 3' peak of RNAP II is due to contributions from the 5' ends of neighboring genes, we filtered out all of the genes that have annotated 5' ends within 1 kb of the 3' peaks, independent of their expression levels. Metagene profiles (**a**) and ratio plots (**b**) look very similar to those generated without the filtering (Figures 3a and 4a). **c** and **d**, Male SL2 cells are, on average, tetraploid. Limiting the analysis to X-linked genes present in two copies and autosomal genes present in four copies (the ideal male X to A ratio in a tetraploid) results in very similar metagene profiles (**c**) and ratio plots (**d**) to Figures 3a and 4a.

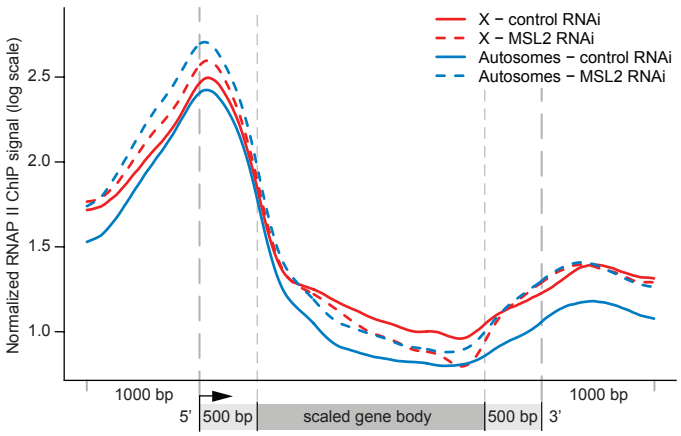

Figure S3. RNAP II ChIP-chip for control RNAi or MSL2 RNAi. RNAP II ChIP-chip was conducted with the 4H8 antibody (Abcam) that recognizes the RNAP II C-terminal domain (CTD) in *Drosophila* SL2 cells. Nimblegen tiling arrays were used that contain the entire chromosome X and the left arm of chromosome 2 (2L) tiled at 100 bp resolution (Alekseyenko *et al*., 2006). Metagene profiles were generated using the same group of long expressed genes used to generate GRO-seq metagene profiles. While the overall profiles are consistent with those obtained by GRO-seq, RNAP II ChIP results have lower sensitivity and resolution, detecting only limited amounts of elongating RNAP II and lacking directionality.

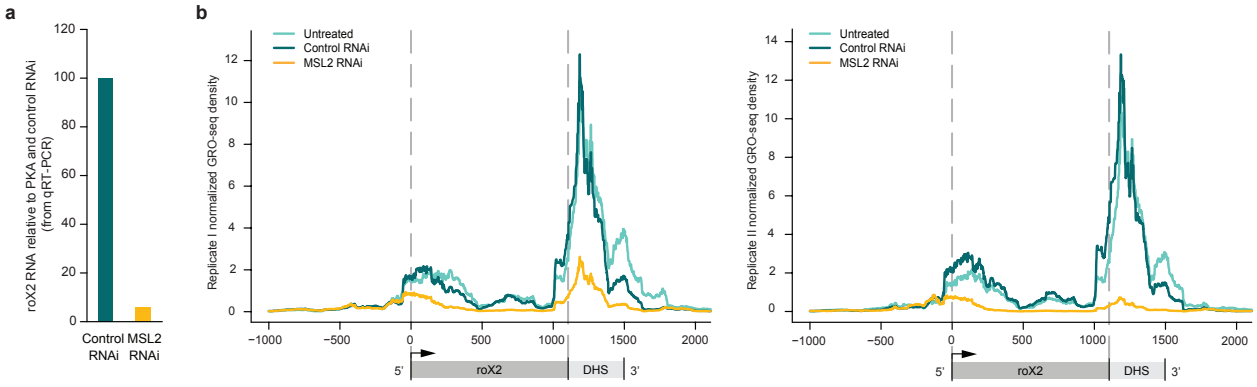

Figure S4. **GRO-seq profiles for the *roX2* gene correlate between replicates. a**, Expression levels of *roX2* for MSL2 RNAi and control RNAi samples, as assayed by qPCR (average of two experiments). **b**, Normalized GRO-seq sense-strand read density within *roX2* for replicate I and replicate II.

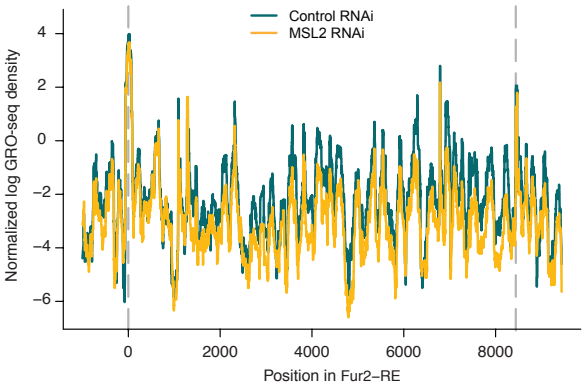
Control RNAi
MSL2 RNAi
Normalized log GRO-seq density
Position in Fur2–RE

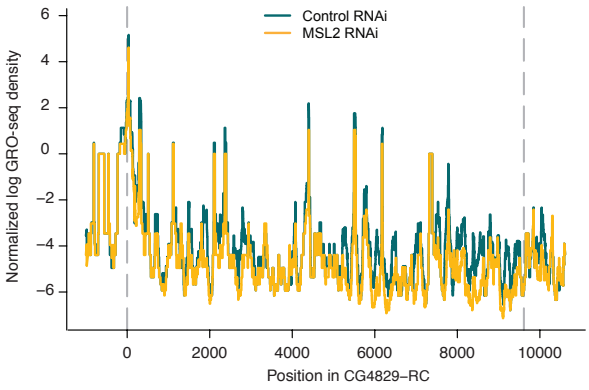
Control RNAi
MSL2 RNAi
Normalized log GRO-seq density
Position in CG4829–RC

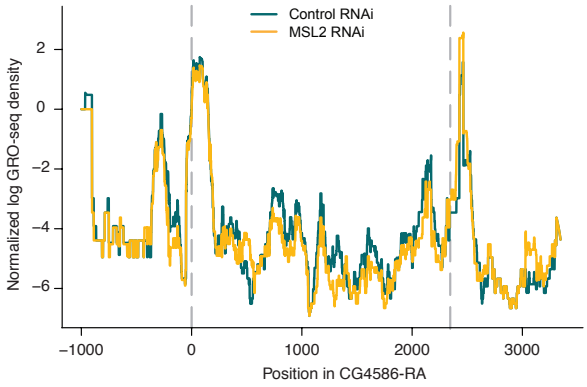
Control RNAi
MSL2 RNAi
Normalized log GRO-seq density
Position in CG4586-RA

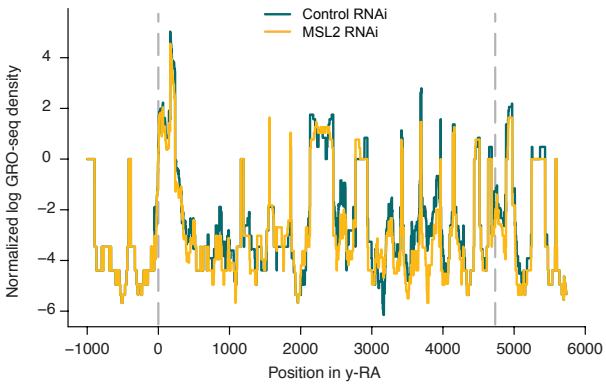
Control RNAi
MSL2 RNAi
Normalized log GRO-seq density
Position in y-RA

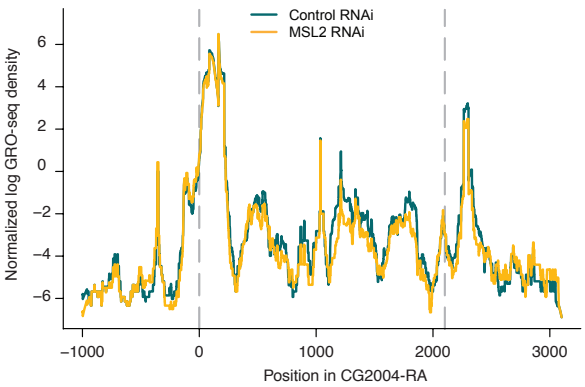
Control RNAi
MSL2 RNAi
Normalized log GRO-seq density
Position in CG2004-RA

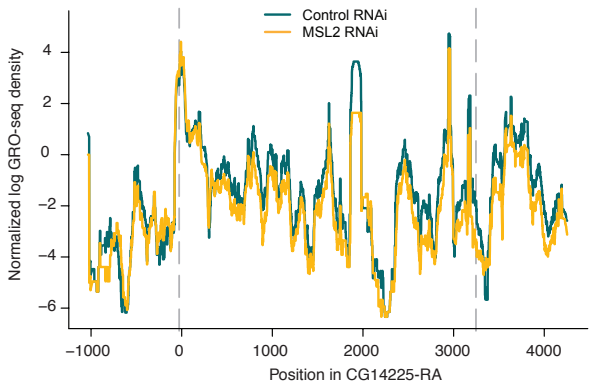
Control RNAi
MSL2 RNAi
Normalized log GRO-seq density
Position in CG14225-RA

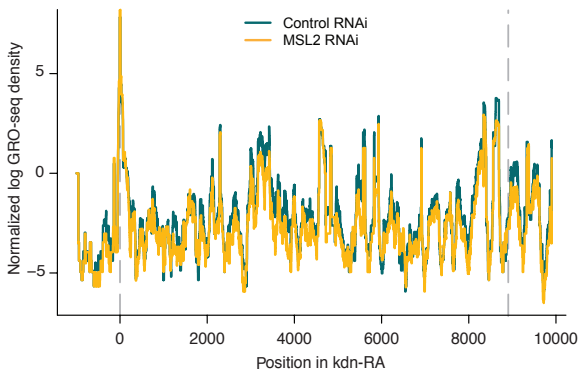
Control RNAi
MSL2 RNAi
Normalized log GRO-seq density
Position in kdn-RA

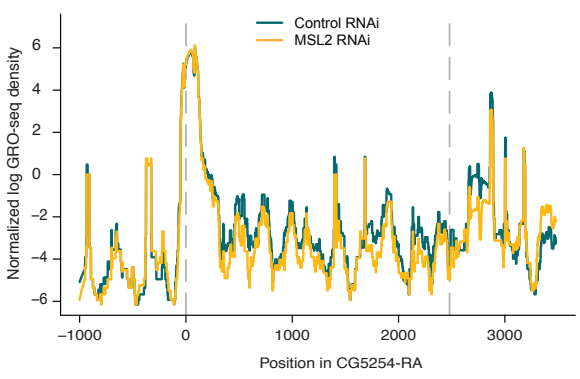
Control RNAi
MSL2 RNAi
Normalized log GRO-seq density
Position in CG5254-RA

(on previous page)

Figure S5. Individual unscaled gene profiles for genes on the X chromosome. Profiles show an alignment of control and MSL2 RNAi GRO-seq density at the 5' end and a divergence that increases across gene bodies (*cf*. Figure S6). The non-uniform nature of the GRO-seq signal over gene bodies may be due to sequence bias by T4 RNA ligase during ligation of RNA linkers onto nascent transcripts (Maĭstrenko *et al*., 1984).

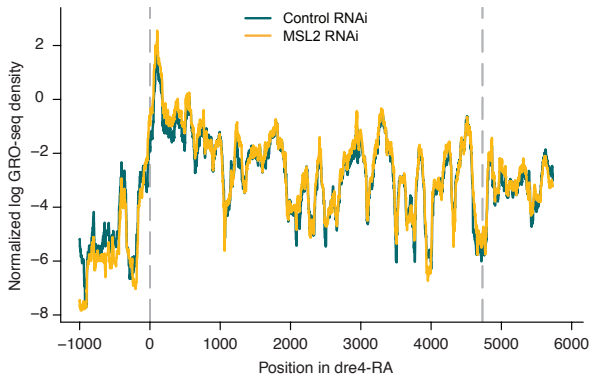
Control RNAi
MSL2 RNAi
Normalized log GRO-seq density
Position in dre4-RA

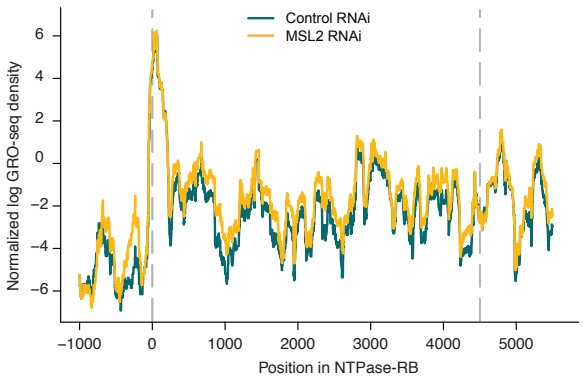
Control RNAi
MSL2 RNAi
Normalized log GRO-seq density
Position in NTPase-RB

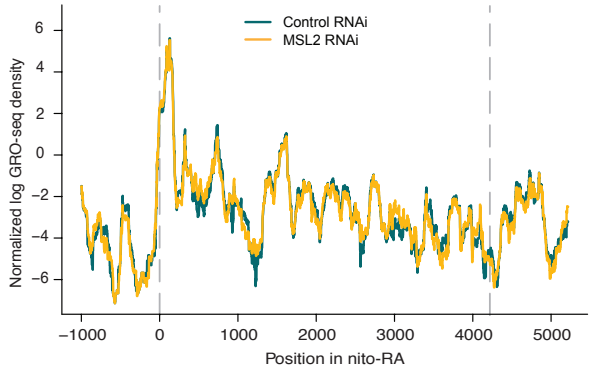
Control RNAi
MSL2 RNAi
Normalized log GRO-seq density
Position in nito-RA

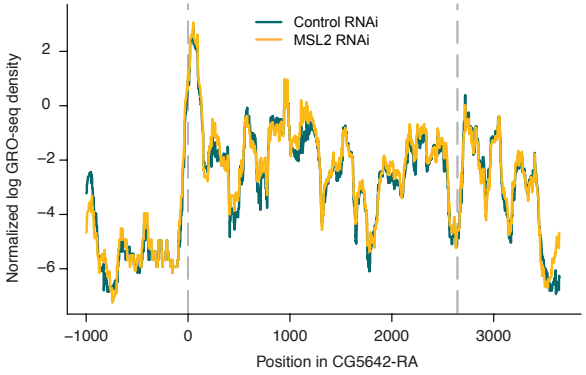
Control RNAi
MSL2 RNAi
Normalized log GRO-seq density
Position in CG5642-RA

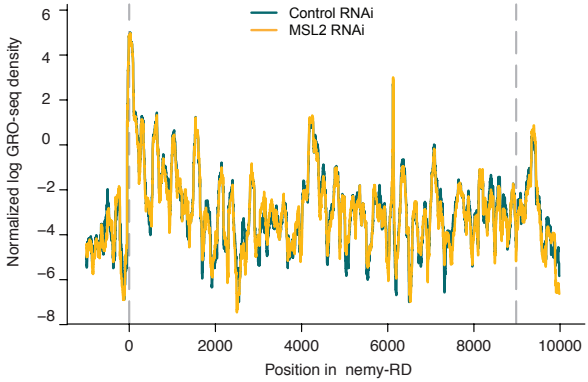
Control RNAi
MSL2 RNAi
Normalized log GRO-seq density
Position in nemy-RD

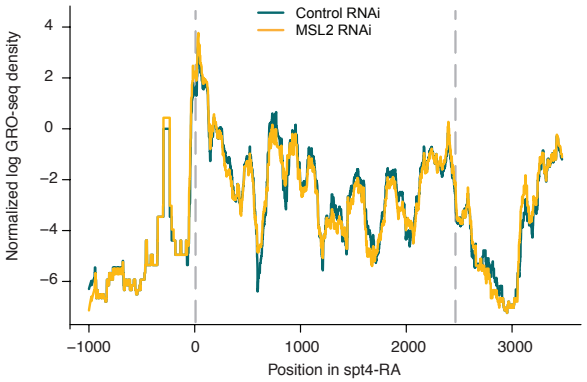
Control RNAi
MSL2 RNAi
Normalized log GRO-seq density
Position in spt4-RA

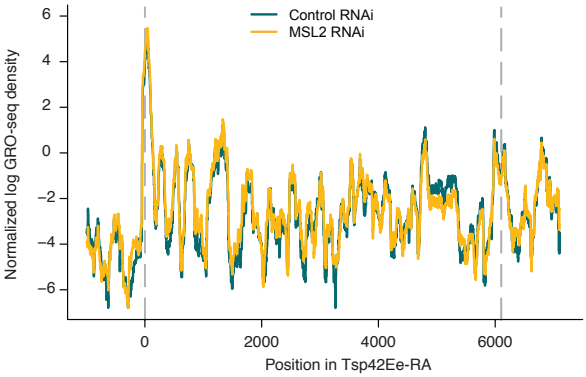
Control RNAi
MSL2 RNAi
Normalized log GRO-seq density
Position in Tsp42Ee-RA

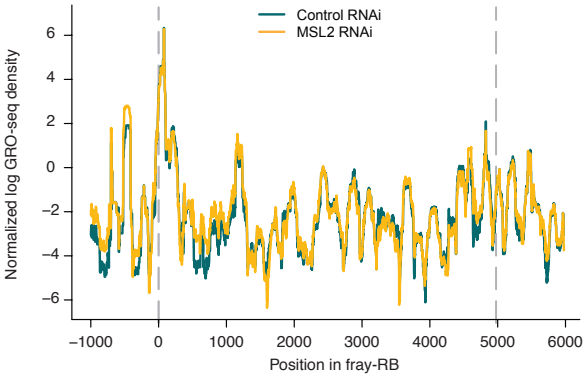
Control RNAi
MSL2 RNAi
Normalized log GRO-seq density
Position in fray-RB

(on previous page)

Figure S6. Individual unscaled GRO-seq profiles for genes on autosomes. Autosomal genes show a strong overlap between control and MSL2 RNAi GRO-seq density.

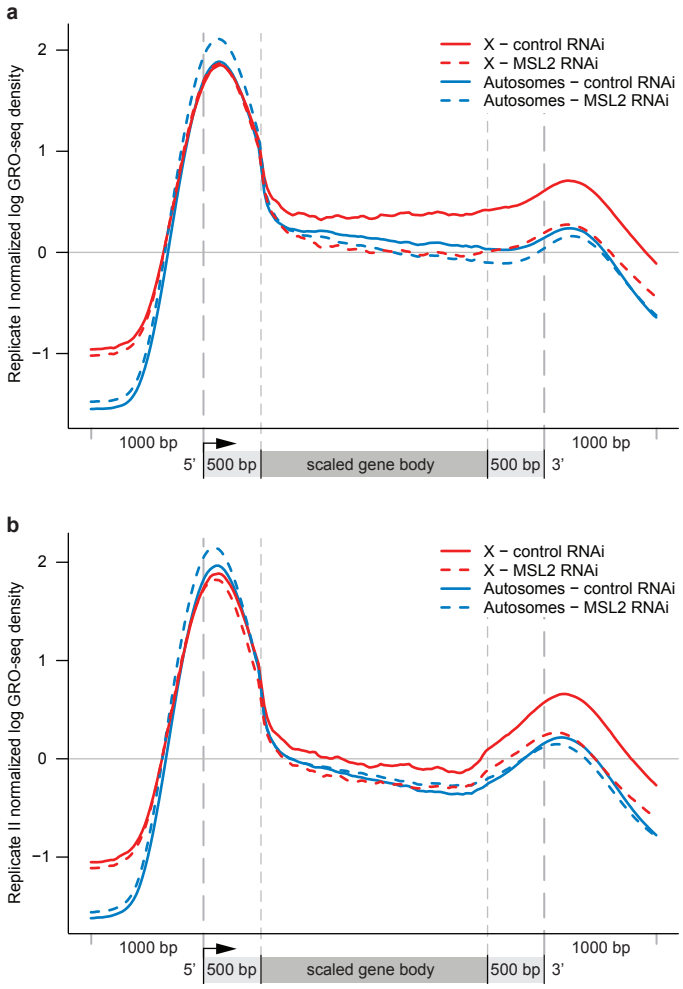

Figure S7. GRO-seq metagene profiles for two replicate experiments. **a**, Replicate I. **b**, Replicate II. In each case, the X is significantly affected within the bodies of genes when compared to autosomes.

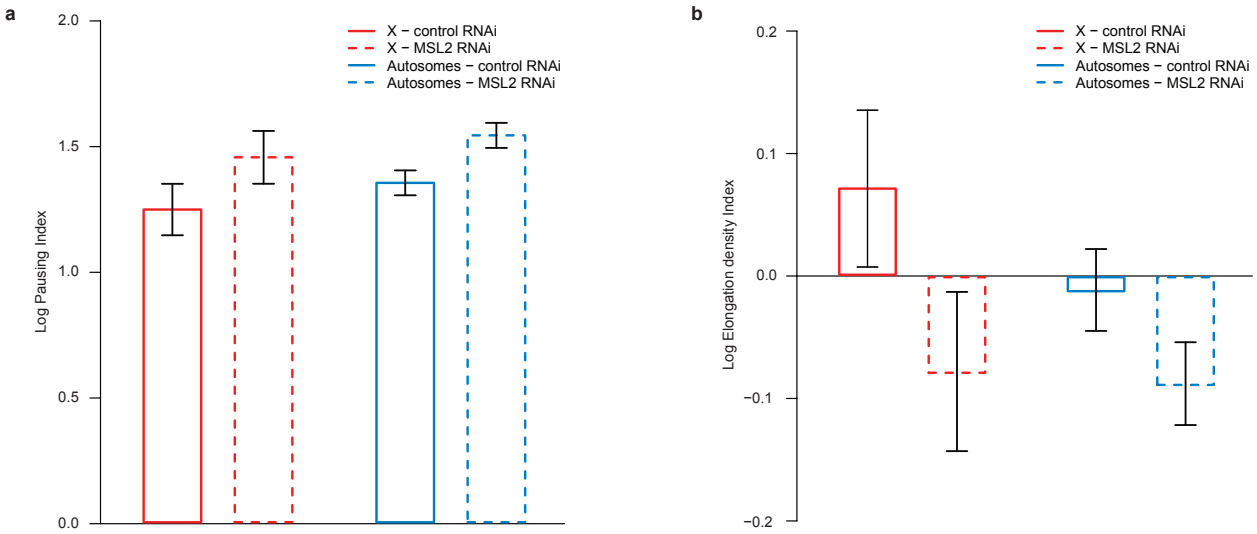

Figure S8. PI and EdI distributions between control RNAi and MSL2 RNAi. **a**, The PI increases after MSL2 RNAi for both the X and autosomes; however, the ratio between control RNAi and MSL2 RNAi is not significantly different for the X and autosomes (Figure 3b). **b**, The EdI decreases after MSL2 RNAi for both the X and autosomes, but the X has a much more significant decrease ($P < 10^{-15}$). The ratios of these values are shown in Figure 3b.

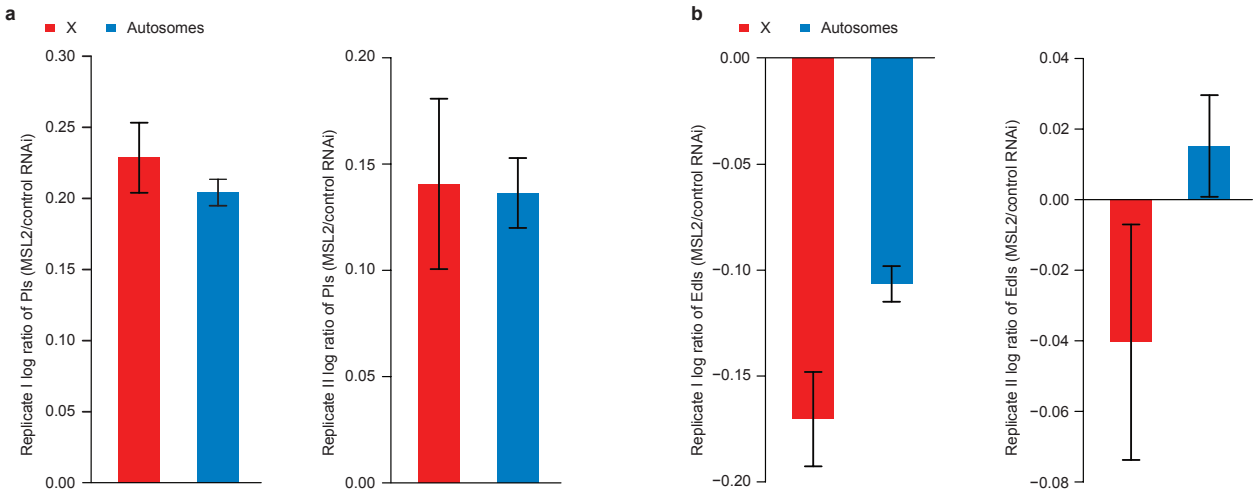

Figure S9. PI and EdI ratios between control RNAi and MSL2 RNAi for each replicate. a, The ratio plots for PI. The ratio change for replicate I shows marginal significance between the X and autosomes, while replicate II, shows no significance. **b**, The ratio plots for EdI. Ratio plots for each individual replicate are shown to demonstrate that MSL2 RNAi clearly affects the EdI more strongly on the X chromosome compared with autosomes in both replicates.

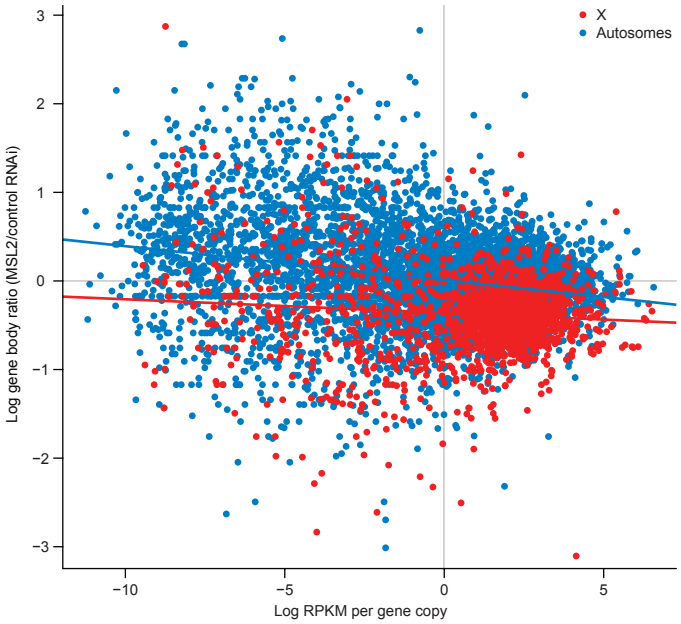

Figure S10. Relative change in tag density after MSL2 RNAi per gene. MSL complex binds to genes independent of their expression level (Alekseyenko *et al*., 2006). Consistent with this previous result, there is not a strong relationship between gene body density change after MSL2 RNAi and GRO-seq read density per gene (measured in reads per kilobase per million of mapped reads (RPKM), per gene copy).

Supplementary Tables

Dividing Point	*P* values X EdI vs Aut. EdI (Untreated)	*P* values X EdI ratio vs Aut. EdI ratio
05%	0.47	**5.8e-07**
10%	0.21	**2.2e-11**
15%	**0.041**	**2.9e-13**
20%	**0.044**	**1.6e-15**
25%	**0.016**	**< 1e-15**
30%	**0.0043**	**< 1e-15**
35%	**0.0016**	**4.0e-15**
40%	**0.0017**	**5.2e-14**
45%	**0.0038**	**1.0e-13**
50%	**0.0076**	**1.2e-13**
55%	**0.0047**	**5.0e-10**
60%	**0.0023**	**3.1e-08**
65%	**0.0010**	**2.6e-08**
70%	**0.0035**	**1.4e-06**
75%	**0.00045**	**0.00016**
80%	**0.00013**	**2.4e-05**
85%	**0.00078**	**0.00011**
90%	**9.5e-05**	**0.0028**
95%	**0.0010**	0.34

Table S1. **Elongation density indices (EdI) differ between genes on the X and autosomes and exhibit MSL-dependence**. Genes were divided at different points along their lengths (column 1). In untreated samples, statistically significant increases in the EdI on the X chromosome compared with autosomes are observed at points upstream of the 3' end (column 2). For this test, H_0: Chr X EdI ≤ Autosome EdI; H_A: Chr X EdI > Autosome EdI. When comparing control and MSL2 RNAi treatments, the EdI is decreased specifically on the X compared with autosomes with statistical significance when genes are divided at points anywhere before 90% (column 3). For this test, H_0: Chr X EdI ratio ≥ Autosome EdI ratio; H_A: Chr X EdI ratio < Autosome EdI ratio. Significant *P*-values are highlighted with a gray background.

Dividing Point	*P* values X EdI vs Aut. EdI (Untreated)	*P* values X EdI ratio vs Aut. EdI ratio
05%	0.47	**3.3e-07**
10%	0.35	**1.2e-10**
15%	0.082	**2.7e-09**
20%	**0.042**	**5.7e-12**
25%	**0.045**	**3.9e-15**
30%	**0.0079**	**3.1e-14**
35%	**0.0026**	**3.1e-12**
40%	**0.0040**	**6.0e-11**
45%	**0.0047**	**4.3e-10**
50%	**0.011**	**1.4e-10**
55%	**0.0088**	**1.5e-07**
60%	**0.0016**	**3.9e-07**
65%	**0.0011**	**1.4e-06**
70%	**0.0017**	**3.1e-05**
75%	**0.00015**	**0.00051**
80%	**8.8e-05**	**0.0013**
85%	**8.8e-05**	**0.00020**
90%	**6.2e-06**	**0.0150**
95%	**2.2e-05**	0.27

Table S2. Significance of changes in the EdI for GRO-seq replicate I. Similar trends are observed as described for Table S1.

Dividing Point	*P* values X EdI vs Aut. EdI (Untreated)	*P* values X EdI ratio vs Aut. EdI ratio
05%	0.43	**0.025**
10%	0.49	**7.4e-05**
15%	0.29	**5.6e-05**
20%	0.20	**3.2e-05**
25%	**0.023**	**0.00011**
30%	**0.0097**	**1.1e-05**
35%	**0.0032**	**2.3e-05**
40%	**0.0036**	**2.9e-06**
45%	**0.0088**	**6.6e-06**
50%	**0.014**	**9.6e-06**
55%	**0.0023**	**2.8e-05**
60%	**0.0011**	**0.00049**
65%	**0.00013**	**9.4e-05**
70%	**0.00032**	**4.4e-05**
75%	**0.0011**	**0.0023**
80%	**0.00050**	**0.0048**
85%	**7.7e-05**	0.066
90%	**0.00015**	0.24
95%	**0.0023**	0.39

Table S3. Significance of changes in the EdI for GRO-seq replicate II. Similar trends are observed as described for Table S1.

Supplemental References

Alekseyenko, A. A., Larschan, E., Lai, W. R., Park, P. J. & Kuroda, M. I. (2006). "High-resolution ChIP-chip analysis reveals that the *Drosophila* MSL complex selectively identifies active genes on the male X chromosome." Genes Dev **20**:848-857.

Maĭstrenko VF, Pustoshilova NM, Kliagina VP, Sedel'nikova EA, Smolianinova OA. 1984. [Substrate specificity of T4 RNA-ligase. The effect of the nucleotide sequence of the minimum phosphate acceptor on the efficacy of intermolecular ligation] Russian. Bioorg Khim. **10**:498-505.